

From the second formula of (2) it follows that

$$\sin \theta = -\frac{k}{\sqrt{c^2 + k^2}} \left(1 - \frac{y}{2k}\right) \pm \sqrt{\frac{y}{2k} \left[1 - \frac{k^2}{c^2 + k^2} \left(1 - \frac{y}{2k}\right)\right]},$$

and since the circulation of the velocity Γ equals the discontinuity of the potential,

$$\Gamma = 4\lambda V \sqrt{c^2 + k^2} \sqrt{\frac{y}{2k} \left[1 - \frac{k^2}{c^2 + k^2} \left(1 - \frac{y}{2k}\right)\right]},$$

the tip of a curved wing is under a smaller load than the tip of a straight wing (Fig. 3, where 1-3 correspond to $k/c = 0, 0.5,$ and 1).

LITERATURE CITED

1. G. I. Maikapar, "Study of the vortex theory of a propeller," Tr. Leningr. Inst. Inzh. Grazhdanskogo Vozdushnogo Flota, No. 21 (1940).
2. A. A. Nikol'skii, "Carrying properties and inductive drag of the wing-fuselage system," Prikl. Mat. Mekh., 21, No. 2 (1957).
3. V. V. Golubev, "Theory of the wing of an aeroplane with finite span," Tr. TsAGI, No. 108 (1931).

EFFECT OF SURFACE POTENTIAL AND INTRINSIC MAGNETIC FIELD ON RESISTANCE OF A BODY IN A SUPERSONIC FLOW OF RAREFIED PARTIALLY IONIZED GAS

V. A. Shuvalov

UDC 533.95:538.4:537.523:550.38

The character of flow over a body, structure of the perturbed zone, and flow resistance in a supersonic flow of rarefied partially ionized gas are determined by the intrinsic magnetic field and surface potential of the body. The effects of intrinsic magnetic field and surface potential were studied in [1-4]. There have been practically no experimental studies of the effect of intrinsic magnetic field on flow of a rarefied plasma. Studies of the effect of surface potential have been limited to the case $R/\lambda_d \lesssim 50$ [1, 3]; this is due to the difficulty of realization of flowover regimes at $R/\lambda_d \gtrsim 10^2$ (where R is the characteristic dimension of the body and λ_d is the Debye radius). At the same time $R/\lambda_d \gtrsim 10^2$, the regime of flow over a large body, is of the greatest practical interest. The present study will consider the effect of potential and intrinsic magnetic field on resistance of a large ($R/\lambda_d \gtrsim 10^2$) axisymmetric body (disk, sphere) in a supersonic flow of rarefied partially ionized gas.

1. Experiments were performed with a plasma aerodynamic tube in a flow of partially ionized gas produced by a gas discharge accelerator with the working material ionized by electron collision. The plasma flow with intensity $j_\infty \approx 10^{15} - 10^{17} \text{ cm}^{-2} \text{ sec}^{-1}$ was fed to the working chamber with residual gas pressure of $\sim 4 \cdot 10^{-5} \text{ Pa}$. The plasma flow parameters in the working chamber at a pressure of $\sim 10^{-3} \text{ Pa}$ were measured by movable electrostatic probes of three types: planar with working surface 3.5 mm in diameter, made of molybdenum, cylindrical probe in thermoanemometer form [5] with working section made of 0.06 mm tungsten wire 6.5 mm long, isolated molybdenum wire probe with diameter 0.04 mm and length 2.3 mm.

Dnepropetrovsk. Translated from Zhurnal Prikladnoi Mekhaniki i Tekhnicheskoi Fiziki, No. 3, pp. 41-47, May-June, 1986. Original article submitted April 17, 1985.

Measurement of probe characteristics and derivatives of probe current were performed automatically. The probe measurement circuits recorded current-voltage characteristics on a recording dc milliammeter operating in conjunction with a photomultiplier, using a resistance box as a reference resistance, and allowed measurements of probe currents in the range $1 \cdot 10^{-7}$ - $1.5 \cdot 10^{-1}$ A with continuously adjustable probe voltage from 0 to 250 V. Uncertainty in measurement of individual current-voltage characteristics did not exceed +2%. Derivatives of probe current with respect to voltage were measured by the harmonic method [6]. Since the probe current derivatives were used only to determine the plasma potential ϕ_0 , no calibration of probe current harmonics was performed.

The plasma potential was determined by the second derivative method, and also from the electron component of the probe characteristic, constructed on a semilogarithmic scale. Moreover, during the course of the experiments plasma noises recorded by the probes were measured, which allowed monitoring the accuracy of plasma potential measurements. Maximum plasma noises corresponded to the space potential. It proved to be the case that the plasma potential found from the current $d^2I_e/dV^2 = 0$ and the noise maximum corresponded better to the beginning of deviation of the semilogarithmic characteristic from linearity than did the point of intersection of the asymptotes. A similar phenomenon was observed in determination of the space potential using the cylindrical probe in thermocouple form, operating as a thermoprobe. The plasma potential was measured using the point of divergence between characteristics of the cold and hot probes. Scattering in plasma potential values did not exceed $\pm 4\%$.

The energy of the flow ions W_i was found from the value of the local plasma potential relative to the source anode. The ion energy values obtained agreed satisfactorily with W_i values obtained using a multielectrode probe-analyzer and the characteristic of the planar probe [7]. Scattering in W_i values did not exceed $\sim \pm 4.5\%$.

In measuring the probe current-voltage characteristics special attention was given to purity of the probe surface. Immediately before measurements the working surfaces of the sensors were washed by a plasma flow and heated to temperatures of ~ 1500 K. The ion component of the probe characteristic was measured beginning at ~ 250 V. Probe working surfaces were purified by the intense bombardment of the ion flux. This eliminated the effect of surface impurities from the probe measurements.

Directed motion did not distort the form of the probe characteristic. The current-voltage characteristics $\log I_e = f(V)$ has a clearly expressed linear segment. This allowed determination of electron temperature T_e by the usual method.

Comparison of charged particle concentration values N_e found for various segments of the electron branch of the cylindrical probe current-voltage characteristic produced a scattering of local N_e values over a 3:1 range [8, 9]. This scattering is caused by uncertainty in choosing the electron probe current I_e corresponding to the plasma potential, and also the difference between the real probe characteristic and an ideal one, due to secondary emission, electron reflection, etc. Therefore to increase the accuracy of the N_e measurements, the uhf-diagnostic method was employed in parallel with the probe method, with an interferometer in the 3 cm range [10]. Local charged particle concentration values N_e calculated for I_e measured by plane and cylindrical probes at the point of the upper asymptote of the characteristic $\log I_e = f(V)$, which corresponds to $\varphi = \varphi_0 (V = \varphi - \varphi_0)$, found at $d^2I_e/dV^2 = 0$, agreed satisfactorily with the uhf-diagnostic results [10].

The isolated cylindrical probe, used for measurement of the rarefield plasma flow parameters, could be rotated about horizontal and vertical axes from 0 to 212° . Vertical and horizontal rotations are necessary to obtain the absolute maximum of the ion current. The ratio $(j_i/j_i^0)_{\max}$ at $\theta = 0$, where $j_i^0 \approx 2aI_n e U_\infty \times (\sin^2 \theta - 2eV/M_i U_\infty^2)^{0.5}$, a is the radius, l is probe length, U_∞ , the mass length of the flow were used in accordance with the cylindrical probe end effect theory [11] to determine the temperature of flow ions [12].

2. The force produced by the rarefied plasma flow on the target depends significantly on the surface potential of the body. For positive target potentials relative to the plasma potential the force applied to the target by a flow of low density partially ionized gas is determined by bombardment of the surface by electrons, fast and slow neutral particles, produced by charge exchange of ions with the residual gas, metastable particles, etc.:

$$F_{V>0} = F_e + F_n + F_0 + F_m + \dots = F_e(V) + \Delta F.$$

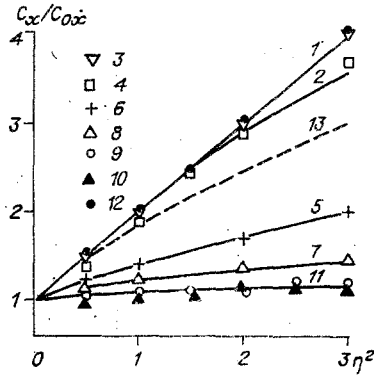


Fig. 1

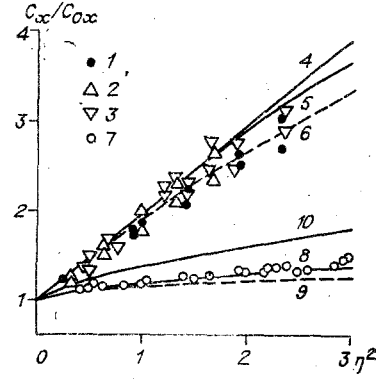


Fig. 2

Here F_e is the pressure produced by electron bombardment, F_n is the contribution of fast neutral particles, F_0 , that of slow neutrals, F_m , that of metastables. At negative potentials the body experiences a pressure produced by bombardment of the surface by ions, neutrals, and metastables:

$$F_{V<0} = F_i + F_n + F_0 + F_m + \dots = F_i(V) + \Delta F$$

(ΔF is independent of target potential).

Considering that the pressure produced by surface bombardment by electrons is much less than that produced by ion bombardment [13], we have

$$\delta F = F_{V<0} - F_{V>0} = F_i - F_e \approx F_i. \quad (2.1)$$

Equation (2.1) permits separation of the contribution of the ion component from the force produced by the rarefied plasma flow on the target.

The targets used were an aluminum sphere ≈ 38 mm in diameter and a disk 43.5 mm in diameter and 1.2 mm thick, oriented perpendicular to the velocity vector of the incident flow. The targets were installed on a compensation type microscale [14, 15] based on the standard magneto-electrical system of a type N359 dc milliammeter. The tracking system employed an F359 photodiode dc amplifier circuit and an N359 recording milliammeter. When the magneto-electric system of the microammeter is used the compensation current passing through the circuit is directly proportional to the applied mechanical moment. To increase sensitivity of the microscale and decrease the contribution of the quantity ΔF to the balance of forces the target holder was placed in a dielectric (glass) tube with inner diameter of ≈ 18 mm. The range of measurable forces with an arm $L \approx 450$ mm comprised $\approx 5 \cdot 10^{-3} - 250$ dyn. Uncertainty of angular location of the target within the flow did not exceed $\pm 20'$.

In measuring the coefficient of lateral resistance of the body the expression

$$C_x \approx (2e/M_i)F_x/I_i U_\infty$$

was used, where F_x is the lateral resistance force of the model; I_i is the ion current.

Measured and calculated dependences of the lateral resistance coefficients of sphere and disk on potential surface for a wide range of the parameters R/λ_d , eV/W_i are shown in Figs. 1, 2, where C_{0x} , the values of the lateral resistance coefficients, at $V = 0$ correspond to free molecular flow conditions for neutral fluxes. Values of C_{0x} measured in a supersonic flow of rarefied partially ionized gas at $U_\infty \approx 10$ km/sec for a sphere were given in Table 1 of [15]. Lines 1, 2 of Fig. 1 show the dependence of C_x/C_{0x} on $\eta^2 = eV/W_i$, obtained by numerical simulation (discrete overflow model) of the interaction between a conductive sphere with $R/\lambda_d \approx 2$ and 14 with a rarefied plasma flow [2]. Similar data from [2] for a disks are illustrated by lines 5, 7.

In [1] the dependence of C_x/C_{0x} on η^2 for a wide range of parameters η^2 and R/λ_d was described by the empirical expression

$$C_x/C_{0x} \approx 1 + [1 - \exp(-3.63\Phi_W^{0.5}/\eta^2 R/\lambda_d)] \eta^2, \quad (2.2)$$

where $\Phi_W = eV/kT_e$. Points 12 and line 13 of Fig. 1 show values of C_x/C_{0x} calculated with Eq. (2.2) for a sphere with $R/\lambda_d \approx 2$, while points 3, 4 are C_x/C_{0x} values calculated for

$R/\lambda_d \approx 2, 14$ with an approximation obtained in the present study,

$$C_x/C_{0x} \approx 1 + [1 - \exp(-\Phi_W^{0.5}/0.263R/\lambda_d)] \eta^2. \quad (2.3)$$

In the range $1 \leq R/\lambda_d \leq 15$ the values of C_x/C_{0x} calculated with Eq. (2.3) agree better with the numerical simulation results of [2] than with Eq. (2.2). Points 6, 8 are calculated values of C_x/C_{0x} for a disk with $R/\lambda_d \approx 2, 14$, found with the empirical approximation of the present study

$$C_x/C_{0x} \approx 1 + [1 - \exp(-\Phi_W^{0.5}/0.3\eta^2R/\lambda_d)] (\sqrt{1 + \eta^2} - 1).$$

Points 9, 10 are experimental C_x/C_{0x} values for the round conductive disk of the present study in flows of rarefied He, Ne, N_2 , Ar, Kr, and Xe plasma. Curve 11 shows calculated C_x/C_{0x} values of a disk for $W_i \approx 60$ eV ($U_\infty \approx 9.4$ km/sec), $T_e \approx 3$ eV, and $R/\lambda_d \approx 117$ in an Xe^+ flow obtained with an empirical approximation used for $R/\lambda_d \gtrsim 50$,

$$C_x/C_{0x} \approx 1 + [1 - \exp(-\Phi_W^{0.5}/0.3R/\lambda_d)] (\sqrt{1 + \eta^2} - 1).$$

The data presented in Fig. 1 illustrate a tendency toward attenuation of the effect of surface potential on C_x/C_{0x} of a conductive disk with increase in the parameter R/λ_d . A similar tendency for the conductive sphere is shown by Fig. 2, where points 1, 2 are experimental results of Fig. 4 of [1], obtained in a flux of Hg^+ ions at $W_i \approx 105; 150$ eV and $R/\lambda_d \approx 10$. Points 3 are data from Fig. 5 of [1] at $R/\lambda_d \approx 10$, line 5 is the numerical results of [2] for a sphere at $R/\lambda_d \approx 14$, 6 is calculated values of C_x/C_{0x} with Eq. (2.2), and 4 is the empirical Eq. (2.3). Points 7 are the experimental data of the present study. Curve 8 corresponds to the approximation

$$C_x/C_{0x} \approx 1 + [1 - \exp(-\Phi_W^{0.5}/0.263R/\lambda_d)] \eta^{2/3},$$

obtained for $R/\lambda_d \gtrsim 50$, which characterizes experimental conditions in an Xe^+ flow for $W_i \approx 65$ eV, $T_e \approx 3$ eV and $R/\lambda_d \approx 102$; 9 is C_x/C_{0x} values calculated with Eq. (2.2); 10 shows numerical results of [13] for mirror reflection of ions in a rarefied plasma flux by the surface of a large sphere.

Comparison of calculated and measured C_x/C_{0x} values for various R/λ_d for the sphere and disk indicate that with increase in R/λ_d decrease in size of the perturbed zone attenuates the effect of body form, surface curvature, and tangential component of the ion velocity [16]; the difference between C_x/C_{0x} values for sphere and disk decreases. In the limit of large R/λ_d C_x/C_{0x} tends to unity.

3. Numerical and experimental studies of flow over an axisymmetrical body and structure of the perturbed zone for a partially ionized rarefied gas [2, 3, 17] indicate that at $R/\lambda_d \gtrsim 10^2$ the dynamic interaction of the body with the flow is characterized by interaction of particles of the incident flow with the face surface of the body. An intrinsic magnetic field changes the flow patterns and structure of the perturbed zone significantly. An experimental study of perturbed zone structure in the vicinity of a sphere at $R/\lambda_d \gtrsim 10^2$ was performed in the working portion of the stream with minimum parameter gradients in the axial and radial directions. A sphere of radius $R \approx 3.1$ cm was placed in an N_2^+ jet with uniform parameter distribution: external magnetic field intensity $H \approx 2$ Oe, i.e., $R/r_i \approx 1 \cdot 10^{-3}$, $R/r_e \approx 1.0$ (where r_α is the Larmor radius of a type α particle), mass velocity $U_\infty \approx 21$ km/sec, charged particle concentration $N_\infty \approx 3.7 \cdot 10^9$ cm $^{-3}$. The source of the body's intrinsic magnetic field was a solenoid with external diameter of 50 mm, internal diameter 20 m, and height of 34 mm. The distributions of the axial and radial-azimuthal components of the solenoid magnetic field intensity are shown in Fig. 6 of [18].

The intensity of the intrinsic magnetic field is such that in the vicinity of the body a region of locally magnetized plasma develops: $r_e \ll R \ll r_i$. To determine the parameters of such a plasma the planar probe in the wake and the cylindrical probe in the wake and at the face surface of the body were oriented perpendicular to the magnetic field intensity and flow velocity vectors. Charged particle density measurements were performed using the ion branch of the probe characteristic [19, 20].

The structure of the perturbed zone about a sphere with intrinsic magnetic field at $S_i = U_\infty/\sqrt{2kT_e/M_i} \approx 4,3$, $R/\lambda_d \approx 126$, $\Phi_W \approx -1,8$ and $T_e/T_i \approx 4$ is shown in Fig. 3, where z is

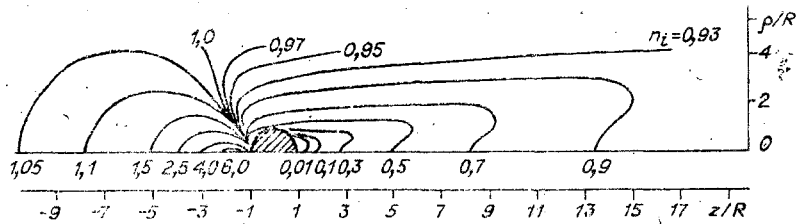


Fig. 3

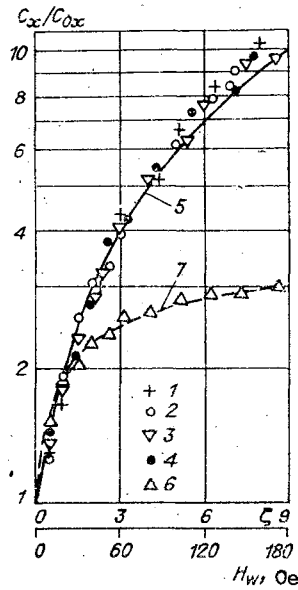


Fig. 4

the distance from the center of the model in the transverse direction, R is the radius of the model, $n_i = I_{iW}/I_i^\infty$ is the ratio of the perturbed ion flow to its unperturbed value in the same section $z/R = \text{const}$. The intrinsic magnetic field intensity vector of the sphere is parallel to the incident flow velocity vector. The structure of the perturbed zone for flow over a disk with intrinsic magnetic field at $R/\lambda_d \gtrsim 10^2$ and $U_\infty \parallel H$ are shown in Fig. 6 of [21].

For flow of a supersonic stream of rarefied partially ionized gas over an axisymmetric object at $R/\lambda_d \gtrsim 10^2$ and $U_\infty \parallel H$ the perturbed zone is characterized by a jet type plasma formation with increased charged particle concentration at the face surface and a region of intense rarefaction in the immediate wake behind the body. Perturbation of the ion component of the supersonic flow with appearance of a weak ($r_e \ll R \ll r_i$) magnetic field in the vicinity of the body is caused by the self-consistent field effect and illustrates the collective nature of the interaction of the rarefied plasma flow with the intrinsic magnetic field of the body.

The character of the flow and elements of the perturbed zone near a body with intrinsic magnetic field at $R/\lambda_d \gtrsim 10^2$ and $U_\infty \parallel H$ (Fig. 6 of [21], Fig. 7a of [18], and Fig. 3 of the present study) indicate that the dynamic interaction of the rarefied plasma flow occurs with the forward surface of the body. This fact has been used in an experimental study of the effect of an intrinsic magnetic field ($U_\infty \parallel H$) on resistance of a large ($R/\lambda_d \gtrsim 10^2$) axisymmetric body: a hemisphere was used as the sensitive element installed on the microscale. The solenoid, mounted on a stationary support, was located inside the sphere, formed from two hemispheres, and in the immediate wake behind the disk. The models used were a disk and a sphere (formed of two hemispheres) made of heavy paper ($R \approx 3.1$ cm). The structure of the perturbed zone for axisymmetric flow over a large ($R/\lambda_d \gtrsim 10^2$) dielectric body with "floating" negative surface potential is identical to the structure of the perturbed zone near a negatively charged conductive sphere (Fig. 1 of [17]) and disk (Fig. 1 of [21]).

The dependence of C_x/C_{0x} on $\xi = \beta e U_\infty P_m / c W_i$ or H_W ($\beta \approx 3,06 \text{ cm}^{-2}$, P_m is the magnetic moment of the solenoid, c is the speed of light, H_W is the magnetic field intensity on the body surface), illustrating the effect of the intrinsic magnetic field on resistance of a large axisymmetric body at $U_\infty |H$ is shown in Fig. 4. Points characterize experimental conditions for a sphere in an N_2^+ flow at $U_\infty \approx 8.2 \text{ km/sec}$ and $N_\infty \approx 3.7 \cdot 10^9 \text{ cm}^{-3}$; 2) $U_\infty \approx 9 \text{ km/sec}$, $N_\infty \approx 1.9 \cdot 10^9 \text{ cm}^{-3}$; 3) $U_\infty \approx 11.7 \text{ km/sec}$, $N_\infty \approx 6.8 \cdot 10^9 \text{ cm}^{-3}$; 4) $U_\infty \approx 12.4 \text{ km/sec}$, $N_\infty \approx 1.8 \cdot 10^9 \text{ cm}^{-3}$. Curve 5 is the empirical relationship $C_x/C_{0x} \approx 1 + 3,06 e U_\infty P_m / c W_i$. The experimental results for a disk in a flow of rarefield N_2 plasma at $U_\infty \approx 12.4 \text{ km/sec}$ and $N_\infty \approx 1.8 \cdot 10^9 \text{ cm}^{-3}$ are shown by points 6. Curve 7 is the approximation $C_x/C_{0x} \approx 1 + (3,06 e U_\infty P_m / c W_i)^{1/3}$.

The data presented indicate that at $U_\infty |H$ particles reflected by the intrinsic magnetic field produce a larger contribution to the forces on an axisymmetric body than particles colliding with the surface. This was also supported by the estimates of [4].

LITERATURE CITED

1. E. Nechtel and W. Pitts, "Experimental study of resistance to motion of satellites caused by electrical forces," *Raket. Tekh. Kosmon.*, 2, No. 6 (1964).
2. M. V. Maslennikov, Yu. S. Sigov, and G. P. Churkina, "Numerical experiments on flow of a rarefied plasma over bodies of various form," *Kosm. Issled.*, 6, No. 2 (1968).
3. G. I. Sapozhnikov, "Experimental studies of an accelerated ion flow and its interaction with models flowed over," *Uchen. Zap. TsAGI*, 2, No. 1 (1971).
4. Yu. F. Gun'ko, G. I. Kurbatova, and B. V. Filippov, "Method for calculation of aerodynamic coefficients of bodies in an intensely rarefied plasma in the presence of an intrinsic magnetic field," in: *Aerodynamics of Rarefied Gases*, 6th ed. [in Russian], Leningrad. Gos. Univ., Leningrad (1973).
5. A. M. Khazen and V. A. Shuvalov, "Determination of the parameters of a partially ionized gas with athermoanemometer," *Zh. Tekh. Fiz.*, 36, No. 2 (1966).
6. V. L. Granovskii, *Electrical Current in a Gas* [in Russian], Gostekhizdat (1952).
7. W. J. Weber, R. J. Armstrong, and J. Trulsen, "Ion-beam diagnostics by means of an electron-saturated plane Langmuir probe," *J. Appl. Phys.*, 50, No. 7 (1979).
8. V. A. Shuvalov, "Determination of charged particle density in a nonequilibrium rarefied plasma from the Langmuir probe characteristic," *Teplofiz. Vys. Temp.*, 10, No. 3 (1972).
9. C. V. Goodall and B. Polychronopoulos, "Measurement of electron density in low density plasma from the electron accelerating region characteristics of cylindrical Langmuir probes," *Planet. Space Sci.*, 22, No. 12 (1974).
10. V. A. Shuvalov, A. E. Churilov, and V. V. Turchin, "Diagnostics of a rarefied plasma jet using the probe and unf-methods," *Teplofiz. Vys. Temp.*, 16, No. 1 (1978).
11. J. R. Sanmartin, "End effect in Langmuir probe response under ionospheric satellite conditions," *Phys. Fluids*, 15, No. 6 (1972).
12. V. A. Shuvalov and V. V. Gubin, "Determination of the degree of nonisothermality of a rarefied plasma flow by probe methods," *Teplofiz. Vys. Temp.*, 16, No. 4 (1978).
13. A. V. Gurevich and A. M. Moskalenko, "Braking of bodies moving in a rarefied plasma," in: *Outer Space Studies* [in Russian], Nauka, Moscow (1965).
14. D. G. Marsden, "Medium sensitivity microscale for measurement of molecular beam pressure forces," *Prib. Nauchn. Issled.*, 39, No. 1 (1968).
15. V. A. Shuvalov, "Transfer of gas ion momentum to the surface of a solid body," *Zh. Prikl. Mekh. Tekh. Fiz.*, No. 3 (1984).
16. A. P. Kuryshv, "Flow over a sphere by a rarefied plasma," in: *Aerodynamics of Rarefied Gases*, 5th Ed. [in Russian], Leningrad. Gos. Univ., Leningrad (1970).
17. V. A. Shuvalov, "Flow over a sphere by nonequilibrium rarefied plasma," *Geomagn. Aeronom.*, 19, No. 6 (1979).
18. V. A. Shuvalov, "Structure of plasma formations at the surface of a cylinder in a flow of partially ionized gas," *Zh. Prikl. Mekh. Tekh. Fiz.*, No. 4 (1984).